広島大学大学院工学研究科研究報告, 55, 1 (2006)
Bulletin of the Graduate School of Engineering, Hiroshima University, Vol. 55, No. 1, 2006

Voltage Control Capability Analysis Based on the Steady State Performance of SVC

Shenghu LI*, Naoto YORINO**, Yoshifumi ZOKA*** and Ming DING****

Static Var Compensator (SVC) is a recent power electronics device that can provide reactive power to control power system voltage. The response speed of SVC is much higher than that of the conventional control devices. In order to fully utilize the capability of SVC, detailed operation characteristics of the SVC must be taken into consideration to improve steady-state stability and steady-state performance. In this paper, the system strength to voltage control is represented as linear contribution of slow-response Var devices to the change of shunt susceptance, which is applied to operation point control while keeping desirable voltage profile. The controllable voltage variation and the feasible slope setting avoiding violation of control limit are quantified based on available control margin at current operation point. The quantitative analysis provides an effective control method of SVC that improves the utilization of its control margin. The paper also discusses coordination among multiple controls of local SVCs.

Key words: Voltage Control, SVC, Operation Point, Steady Voltage Characteristic, Slope

1. Introduction

Compared with fixed or mechanically switched capacitor and reactor, static Var compensators (SVC), such as shunt connected thyristor switched capacitor (TSC) and thyristor controlled reactors (TCR), or fixed capacitor (FC) and TCR, provides fast voltage control, resulting into better steady-state and dynamic performance of power system[1-2]. The steady-state analysis to SVC is usually implemented by adding equivalent SVC models to power flow programs, such as generator model with constant reactive power limits, PVB bus model with shunt susceptance limits, variant shunt suscepatnce model, and variant firing angle model [3-5]. The steady-state characteristics of SVC, such as the original operation point, the voltage deadband to avoid excessive operation, and the control slope, are usually simplified. The voltage deadband is reduced to fixed compensation object, the original operation point is assumed with regulated current or susceptance, and the slope is neglected, although it is concluded that the representation of SVC slope may be more important than the representation for generator voltage regulation. Based on these simplifications rated control margin is always available before disturbances, and the power flow result is more suitable for special snapshots instead of continuous operation. Little attention is given to the successive analysis and control to operation point of SVC[6], such as:

(1) How to make schemes to restore operation point to or close to the regulated value while keeping desirable voltage for future control,
(2) Approximately how much voltage variation may be compensated within SVC control limit,
(3) How to set slope feasibly to better utilize its

* Post-Doctoral Researcher, Artificial Complex Systems Engineering, Hiroshima University
** Professor, Artificial Complex Systems Engineering, Hiroshima University
*** Research Associate, Artificial Complex Systems Engineering, Hiroshima University
**** Professor, Electrical Engineering and its Automation, Hefei University of Technology, China

control margin and coordinate with other Var devices.

In this paper the post-disturbance behavior of SVC is studied and compared with PVB-bus based power flow model. It is found in many cases SVC may operate at non-regulated point with Var output. If detailed steady-state characteristics are included, the original operation point has much effect on SVC capability for voltage control. The previous power flow models simulate more of the dynamic than the steady-state performance after disturbance. Then steady-state operation point control based on the linear expression of Var output, bus voltage, and shunt susceptance is proposed to slowly restore SVC operation point while keeping desirable voltage profile. Controllable voltage variation and feasible slope setting is quantified based on available control range of SVCs and system performance. Although the models and the results are mainly designed for under-voltage control, they may also be easily applied for overvoltage control.

2. SVC Performance after Disturbances

2.1 Post-disturbance performance of SVC

SVC reaction to voltage sag from time t_0 is shown in Fig. 1, where V_i is the bus voltage, V_{refmin}, V_{refmax} are the lower and the upper referenced voltage, $B_{sh,i}$, B_{shset} are the shunt susceptance and its regulated value, B_{shmin}, and B_{shmax} inductive and capacitive susceptance limit of the shunt path including SVC and the step-down transformer. After disturbance, $B_{sh,i}$ is increased by SVC controller to restore the load voltage to V_{refmin}. The operation point at time t_1 may be "a" and "c", or "b" and "d" in Fig.1. Then the slow-response reactive power devices, such as synchronous generators, condensers, mechanically switched capacitor and reactors operated by under- and over- voltage relays, as well as the necessary load shedding executed by load shedding relays, slowly reduce SVC output to (or close to) the regulated susceptance (or regulated current I_{set}) for future fast control, while improving load voltage to a desired value. This process is called operation point control or Var reserve control.

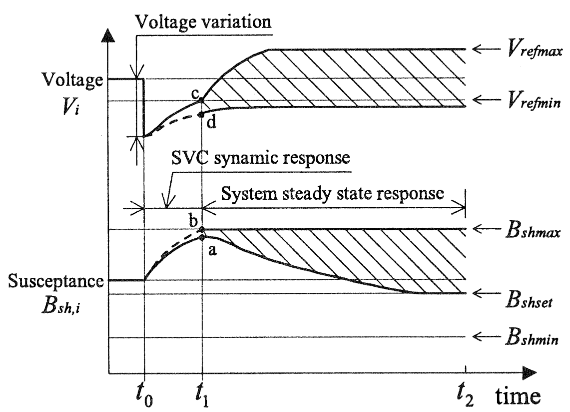

Fig. 1 Post-disturbance reaction of SVC to voltage drop.

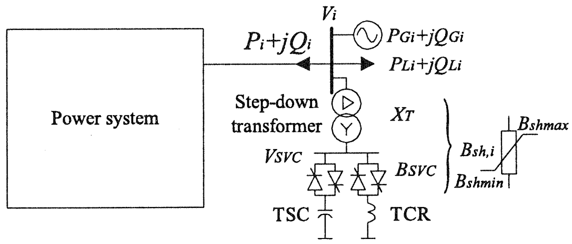

Fig. 2 SVC compensated bus for power flow analysis.

$$
\begin{aligned}
V_{Li} &= V_{refmin}, \quad B_{sh,i} \le B_{shmax} \\
V_{Li} &< V_{refmin}, \quad B_{sh,i} = B_{shmax}
\end{aligned} \tag{1}
$$

In literatures for steady-state analysis, SVC is simulated by generator model or PVB bus model. As shown in Fig. 2, PVB bus model is based on an imaginary PV-bus constrained by (2)-(4), where Q_i is the power injection from the bus to the system and subjected to the lower and the upper limits Q_{imin} and Q_{imax}, Q_{Gi} and Q_{Li} are reactive generation and reactive load. When $B_{sh,i}$ reaches B_{shmin} or B_{shmax}, the bus changes to be a PQ bus, and $B_{sh,i}$ is fixed at B_{shmin} or B_{shmax} with necessary modification to admittance matrix (5).

$$Q_{imin} \le Q_i \le Q_{imax} \tag{2}$$

$$
\begin{aligned}
Q_{imax} &= Q_{Di} + B_{shmax} V_i^2 \\
Q_{imin} &= Q_{Di} + B_{shmin} V_i^2
\end{aligned} \tag{3}
$$

$$Q_{Di} = Q_{Gi} - Q_{Li} \tag{4}$$

$$\Delta Y_{ii} = B_{shi} \tag{5}$$

For a regional system including a SVC compensated bus, the compensated voltage and the shunt susceptance are shown in Fig. 3 by a Newton power flow program, where the referenced voltage is 0.95 pu and 0.98 pu respectively. The power flow results corresponds to either constant voltage or susceptance limit at bus i. It actually simulates more of the dynamic performance instead of the steady-state performance especially when

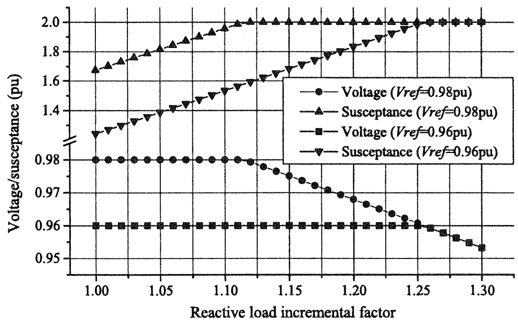

Fig. 3 PVB-bus based power flow results.

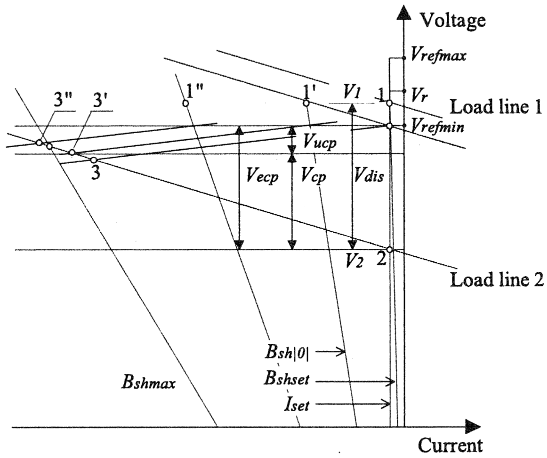

Fig. 4 Steady state V-I characteristic of SVC.

the control limit is not reached. Based on the following assumptions, it tries to make full use of SVC after the disturbance, leaving little margin for future fast voltage control, and making little effort to control the operation point for better performance.

- The referenced voltage (control object), i.e. the voltage setting for the PV bus, is fixed.
- Rated control range for the shunt path is available and independent of operation point before disturbance.
- The slope is not included in the model, therefore no special measure is taken to prevent SVC from reaching the control limits too easily and to coordinate multiple local SVCs.
- The contribution to voltage control from the slowly-response reactive-power devices is not quantitatively simulated.

2.2 Effect of SVC operation point to voltage control

In actual operation, SVC may work as a regular Var device with output for a period of time, such as:

- There is no sufficient Var support from the system due to Var capacity or transmission security/economics.
- For long extra/ultra high voltage transmission under light load conditions, since it's difficult to absorb the redundant reactive power by generators, SVC has to provide inductive output to restrain the overvoltage.

The steady-state V-I characteristic of SVC include the voltage deadband, the regulated susceptance, and the slope, all related to the operation point. A deadband between lower and upper referenced voltage V_{refmin} and V_{refmax} is set to avoid excessive operation of SVC during steady-state operation. After fast voltage control, the operation point control drives SVC to operation point to (close to) regulated susceptance to keep sufficient margin for future fast control.

The slope prevents SVC from reaching its control limits too easily, and makes it possible to coordinate output among multiple local SVCs. It is defined as the ratio of voltage-magnitude change to current-magnitude change over the linear-control range, where I_{SVC} and I_{sh} are the same currents at the shunt path.

$$k_{sl} = \frac{\Delta V}{\Delta I_{SVC}} = \frac{\Delta V}{\Delta I_{sh}} \tag{6}$$

As shown in Fig. 4, when disturbance, such as load increase or transmission contingency, drives operation point from 1 to 2, the voltage drop V_{dis} is quantified by the vertical distance between 1 and 2 (7). The total expected compensation V_{ecp} in steady-state operation may be defined by (8). The final operation point 3 is decided by the intersection of slope with load line which is actually the static voltage characteristic of the system. Actual compensated voltage V_{cp} is equal to V_{ecp} minus the uncompensated voltage V_{ucp} due to slope setting (9).

$$V_{dis} = V_1 - V_2 \tag{7}$$

$$V_{ecp} = V_{ref\min} - V_2$$
$$V_{ecp} = V_1 - V_2 \tag{8}$$

$$V_{cp} = V_{ecp} - V_{ucp} = V_{ecp} - k_{sl} I_{SVC} \tag{9}$$

If the original operation point is 1', the same disturbance will drive the operation point to 3' with larger V_{cp} but near to the control limit. When the

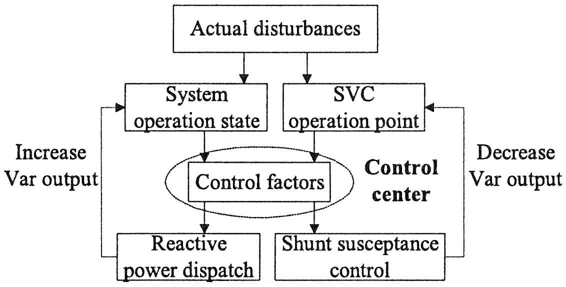

Fig. 5 Schematic design to operation point control.

original point is 1", the intersection of the slope and load line crosses the control limit, and the operation point moves along the control limit with smaller actual compensation. It shows when the slope is included, the steady-state performance of SVC is dependent on its original operation point. Detailed analysis to operation point is helpful to quantify and better utilize the SVC control margin in continuous operation environments.

3. Operation Point Control

Steady-state analysis and control to SVC is usually locally or remotely decided by the control center and implemented by the SVC controller. The control object is to better utilize control margin under different operation conditions. Operation point control after disturbances is discussed in this section, and feasible slope setting is discussed in next section.

As shown in Fig. 5, to restore operation point of SVC for future fast voltage control, the control center decreases SVC output by slowly increasing the Var output of slow-response devices and avoiding fast regulation of SVC. Therefore in the process of operation point control, slope may be neglected and the SVC compensated bus is seen as a PQ bus with a shunt path. The problem now is to find the location and amount of Var output for a prescribed SVC output (shunt susceptance) while keeping desirable voltage profile.

Linearized power flow model is shown in (10)-(11), where ΔP and ΔQ are the changes of active and reactive power, P^{SP} and Q^{SP} are the specified active and reactive powers, $\Delta\theta$ and ΔV are the changes of voltage angle and magnitude, and $J_{P\theta}$, J_{PV}, $J_{Q\theta}$, J_{QV} are the sub-Jacobian matrices[7]. To study the impact of reactive power change to voltage control, the active power is assumed constant, and the reduced Jacobian matrix J_R, or inverse matrix K, is found to establish the incremental relationship between Var injection and bus voltage at given operation point (12)-(16). It partly quantifies the static voltage characteristic of the system.

$$\begin{bmatrix} \Delta P \\ \Delta Q \end{bmatrix} = \begin{bmatrix} J_{P\theta} & J_{PV} \\ J_{Q\theta} & J_{QV} \end{bmatrix} \begin{bmatrix} \Delta\theta \\ \Delta V \end{bmatrix} \tag{10}$$

$$\begin{aligned} \Delta P &= P^{SP} - P \\ \Delta Q &= Q^{SP} - Q \end{aligned} \tag{11}$$

$$\Delta Q = J_R \Delta V \tag{12}$$

$$J_R = J_{QV} - J_{Q\theta} J_{P\theta}^{-1} J_{PV} \tag{13}$$

$$\Delta V = K \Delta Q \tag{14}$$

$$K = J_R^{-1} = (\kappa_{ij}) \tag{15}$$

$$\Delta V_i = \sum_{j\in PQ} \left(\kappa_{ij} \Delta Q_j\right) \tag{16}$$

Since Q_j may be Var injection from generator, load, and SVCs, their contributions to voltage change are separately expressed (17)-(19). By combining the terms with ΔV_i, the voltage change with respect to control variables is found and subjected to shunt susceptance limit (20)-(22), where α, β, γ are control factors. If j is not a SVC compensated bus, $B_{sh,j}$ and $\Delta B_{sh,j}$ are zero. When there is more than one SVC connecting at a bus, they are equaled to one SVC by combining their shunt susceptance. The equations quantify the contributions of system and other SVCs to compensated voltage. If the expected voltage is fixed, the necessary Var increase to reduce SVC output may be found based on slow and continuous linear control. The model is suitable for both capacitive and inductive operation state of SVC.

$$\Delta Q_j = \Delta Q_{Dj} + \Delta Q_{sh,j} \tag{17}$$

$$\Delta Q_{sh,j} = \Delta\left(B_{sh,j} V_j^2\right) \approx V_j^2 \Delta B_{sh,j} + 2B_{sh,j} V_j \Delta V_j \tag{18}$$

$$\Delta V_i = \sum_{j\in PQ} \left(\kappa_{ij} \Delta Q_{Dj}\right) + \sum_{j\in PQ} \left(\kappa_{ij} \Delta Q_{sh,j}\right) \tag{19}$$

$$\begin{aligned} \Delta V_i &= \frac{\sum\limits_{j\in PQ} \kappa_{ij}\left(\Delta Q_{Dj} + V_j^2 \Delta B_{sh,j}\right) + \sum\limits_{\substack{j\in PQ \\ j\neq i}} 2\kappa_{ij} B_{sh,j} V_j \Delta V_j}{1 - 2\kappa_{ii} B_{sh,i} V_i} \\ &= \sum_{j\in PQ} \left(\alpha_{ij} \Delta Q_{Dj}\right) + \sum_{j\in PQ} \left(\beta_{ij} \Delta B_{sh,j}\right) + \sum_{\substack{j\in PQ \\ j\neq i}} \left(\gamma_{ij} \Delta V_j\right) \end{aligned} \tag{20}$$

$$\left.\begin{aligned}\alpha_{ij} &= \frac{\kappa_{ij}}{1-2\kappa_{ii}B_{sh,i}V_i}\\ \beta_{ij} &= \frac{\kappa_{ij}V_j^2}{1-2\kappa_{ii}B_{sh,i}V_i}\\ \gamma_{ij} &= \frac{2\kappa_{ij}B_{sh,j}V_j}{1-2\kappa_{ii}B_{sh,i}V_i}\end{aligned}\right\} \tag{21}$$

$$0 \le \Delta B_{sh,j} \le B_{shmax,j} - B_{sh,j} \tag{22}$$

4. Controllable Range and Slope Setting

Based on SVC operation point, static voltage characteristic of the system, and the possible disturbance, the controllable voltage variation and the feasible slope setting within the control margin may be quantified as shown in Fig. 6.

By neglecting the performance of slow-response devices and remote SVCs in the fast voltage control, and assuming matrix K insensitive to small change of operation point, the actual compensation $V_{cp,i}$ is expressed as:

$$V_{cp,i} \approx \beta_{ii}\Delta B_{sh,i} \tag{23}$$

The uncompensated voltage $V_{ucp,i}$ due to the slope is defined by the change of shunt suscepatnce, instead of change of shunt current, as shown in (24)-(27), where δ_i is the contribution factor of shunt susceptance to bus voltage.

$$V_{ucp,i} = k_{sl,i}\Delta I_{SVCi} = k_{sl,i}\Delta I_{sh,i} \tag{24}$$

$$I_{sh,i} = B_{sh,i}V_i \tag{25}$$

$$\Delta I_{sh,i} \approx V_i\Delta B_{sh,i} + B_{sh,i}\Delta V_i = V_i\Delta B_{sh,i} - B_{sh,i}V_{ucp,i} \tag{26}$$

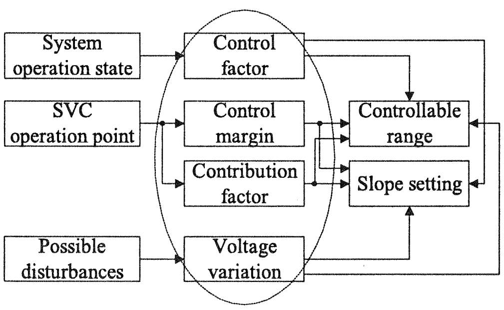

Fig. 6 Schematic design to feasible slope setting.

$$V_{ucp,i} = \frac{k_{sl,i}V_i}{1+k_{sl,i}B_{sh,i}}\Delta B_{sh,i} = \delta_i\Delta B_{sh,i} \tag{27}$$

The total expected compensation $V_{ecp,i}$ within available control margin $\Delta B_{sh,i}$ is based on the change of shunt susceptance (28). The feasible slope setting without violation of control limit is shown in (29), dependent on available control margin and static voltage characteristics of the system.

$$\begin{aligned}V_{ecp,i} &= (\beta_{ii}+\delta_i)\Delta B_{sh,i}\\ &= \left(\beta_{ii} + \frac{k_{sl,i}V_i}{1+k_{sl,i}B_{sh,i}}\right)\Delta B_{sh,i}\end{aligned} \tag{28}$$

$$k_{sl,i} = \frac{V_{ecp,i} - \beta_{ii}\Delta B_{sh,i}}{V_i\Delta B_{sh,i} - B_{sh,i}\left(V_{ecp,i} - \beta_{ii}\Delta B_{sh,i}\right)} \tag{29}$$

When there is more than one SVC, e.g. M SVCs, at bus i with different slope, operation point and control limit, the uncompensated voltage $V_{ucp,i}$ and the total compensation is shown in (30)-(32), and feasible slope setting for j-th SVC, is shown in (33)-(34), all subjected to the control limit. Equation (29) and (33) show that the control margin may be effectively utilized by coordination of slope setting between SVC and the system and among multiple local SVCs.

$$\begin{aligned}V_{ucp,i} &= \sum_{m=1}^{M} k_{sl,m}\Delta I_{sh,m} = V_i\frac{\sum_{m=1}^{M}\left(k_{sl,m}\Delta B_{sh,m}\right)}{1+\sum_{m=1}^{M}\left(k_{sl,m}B_{sh,m}\right)}\\ &= \sum_{m\in i}\delta_m\Delta B_{sh,m}\end{aligned} \tag{30}$$

$$\delta_{im} = \frac{V_i k_{sl,m}}{1+\sum_{m=1}^{M}\left(k_{sl,m}B_{sh,m}\right)} \tag{31}$$

$$V_{ecp,i} = \beta_{ii}\sum_{m=1}^{M}\Delta B_{sh,m} + \sum_{m=1}^{M}\left(\delta_{im}\Delta B_{sh,m}\right) \tag{32}$$

$$k_{sl,j} = \frac{\Psi + \Psi\sum_{m\neq j}\left(k_{sl,m}B_{sh,m}\right) - V_i\sum_{m\neq j}\left(k_{sl,m}\Delta B_{sh,m}\right)}{V_i\Delta B_{sh,j} - B_{sh,j}\Psi} \tag{33}$$

$$\Psi = V_{ecp,i} - \beta_{ii}\sum_{m=1}^{M}\Delta B_{sh,m} \tag{34}$$

5. Numerical Analysis

IEEE 14-bus test system is adopted to validate the control effect. The original capacitor at bus 9 is replaced by a SVC at bus 14. For the base operation condition in

Table I, the control factors $\alpha_{14,i}$, $i = 2, \ldots, 14$, defined in (21) are shown in Fig. 7, where the last column is control factor $\beta_{14,14}$ for the shunt susceptance at bus 14. The Var output of generator at bus 6 is adopted to control shunt susceptance from 0.0688 pu to 0.0088 pu with expected voltage increment ΔV_{14}, where $B_{sh,14}$ = 0.0688 pu, $B_{shmax,14}$ = 0.1 pu, $\alpha_{14,6}$ = 0.2278, $\beta_{14,14}$ = 0.4008. The control error is defined as the voltage difference at bus 14 before and after the control. The control process with expected voltage of 0.95 pu is shown in Fig. 8. The control error increases with Var increase, with the maximum value of 4×10^{-4} pu.

$$\Delta V_{14} = \alpha_{14,6}\Delta Q_{D6} + \beta_{14,14}\Delta B_{sh,14} \qquad \text{(pu)}$$

$$\begin{aligned}\Delta Q_{D6} &= \left(\Delta V_{14} - \beta_{14,14}\Delta B_{sh,14}\right)/\alpha_{14,6} \\ &= 4.3898\Delta V_{14} - 1.7594\Delta B_{sh,14} \qquad \text{(pu)}\end{aligned}$$

When all the reactive load increase 20 %, voltage at bus 14 is 0.9329 pu and the shunt path reaches its limit 0.1 pu. Control factors are shown in Fig. 9, where $\alpha_{14,6}$ = 0.2432, $\beta_{14,14}$ = 0.4076. The control process in Fig. 10 is based on two steps. In the 1st step, the var output of the generator is increased to restore the bus voltage from 0.9329 pu to the reference value (0.95 pu). In the 2nd step the shunt susceptance is restored to the reference value (0.01 pu). The maximum control error for the whole process is 3.6×10^{-3} pu.

$$\Delta Q_{D6} = 4.1118\Delta V_{14} - 1.6759\Delta B_{sh,14} \qquad \text{(pu)}$$

Fig. 11 shows the expected compensation, the actual compensation, and the uncompensated voltage with fixed available shunt susceptance but different slope setting. The uncompensated voltage is nearly proportional to the slope.

$$V_{ecp,14} = \left(\beta_{14,14} + \frac{k_{sl,14}V_{14}}{1 + k_{sl,14}B_{sh,14}}\right)\Delta B_{sh,14}$$

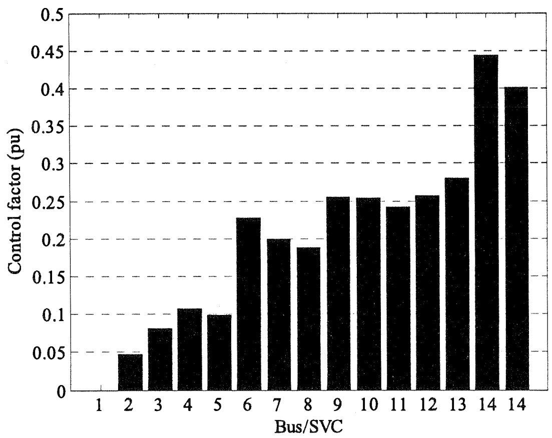

Fig. 7 Control factors under base operation states.

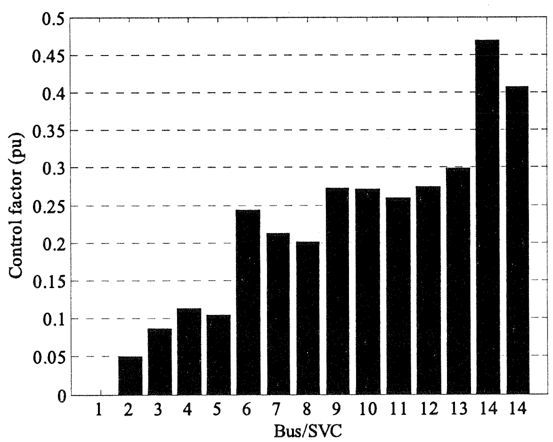

Fig. 9 Control factors under stressed operation states.

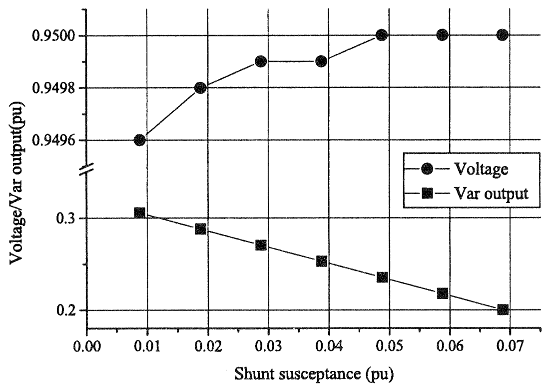

Fig. 8 Operation point control under base operation states.

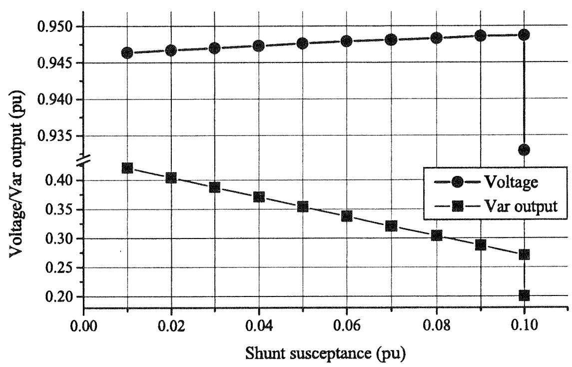

Fig. 10 Operation point control under stressed operation states.

$$\Delta B_{sh,14} \le B_{sh\max,14} - B_{sh,14} = 0.0312 \qquad \text{(pu)}$$

$$V_{ecp,14} \le 0.0125 + 0.02964 k_{sl,i} / \left(1 + 0.0688 k_{sl,i}\right) \quad \text{(pu)}$$

Based on available control margin, the slope should be set no less than the following value to avoid arrival to the control limit. Since physically the slope is set within 1-10 % (typically 3-5 %), the feasible slope setting without violating the control limit is shown in Fig. 12.

$$k_{sl,14} = \frac{V_{ecp,14} - \beta_{14,14}\Delta B_{sh,14}}{V_{14}\Delta B_{sh,14} - B_{sh,14}\left(V_{ecp,14} - \beta_{14,14}\Delta B_{sh,14}\right)}$$

$$k_{sl,14} \ge \frac{V_{ecp,14} - 0.0125}{0.0305 - 0.0688 V_{ecp,14}}$$

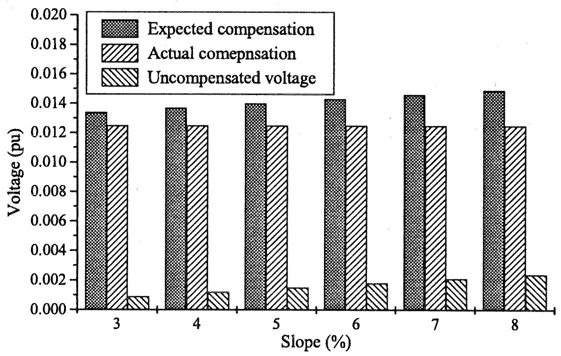

Fig. 11 Available compensation with different slope setting.

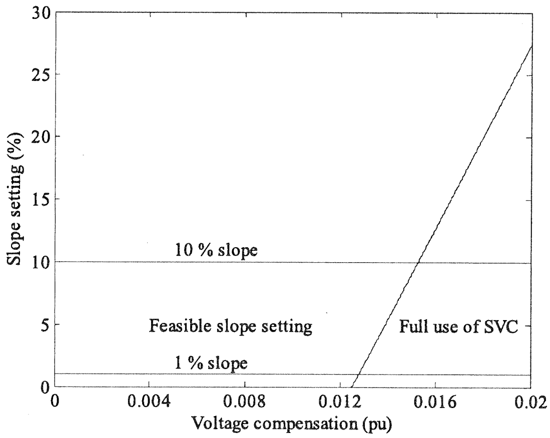

Fig. 12 Slope setting with fixed available control margin.

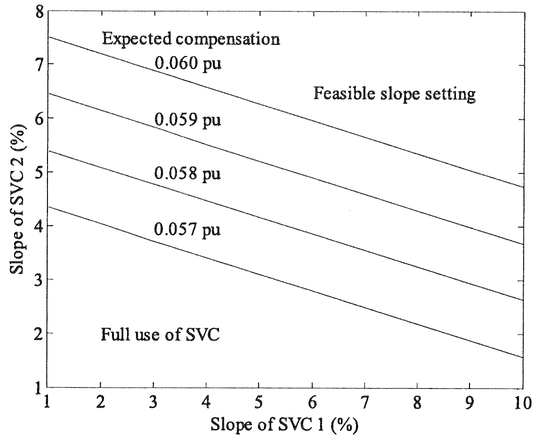

Fig. 13 Slope setting for coordination between two SVCs.

If there is a reserve SVC at bus 14 with a same control limit of 0.1 pu but no output before disturbance (signed at the second SVC at bus 14), the expected compensation is defined by the slope setting of two SVCs, as shown in Fig. 13. It is found the when one SVC produces less Var with a larger slope, the other has to produces more Var with a smaller slope. With the increase of the expected compensation, the feasible slope setting decreases while the possibility of full use of SVCs increases.

$$V_{ecp,i} = \beta_{ii}\left(\Delta B_{sh,1} + \Delta B_{sh,2}\right) + V_i \frac{\left(k_{sl,1}\Delta B_{sh,1} + k_{sl,2}\Delta B_{sh,2}\right)}{1 + \left(k_{sl,1}B_{sh,1} + k_{sl,2}B_{sh,2}\right)}$$

$$= 0.4008\left(\Delta B_{sh,1} + \Delta B_{sh,2}\right) + 0.95 \frac{k_{sl,1}\Delta B_{sh,1} + k_{sl,2}\Delta B_{sh,2}}{1 + 0.0688 k_{sl,1}}$$

$$\le 0.052585 + \frac{0.02964 k_{sl,1} + 0.095 k_{sl,2}}{1 + 0.0688 k_{sl,1}} \qquad \text{(pu)}$$

6. Conclusions

In existing steady-state analysis it is often assumed that SVC works with full rated control range available at any time before disturbance. In this paper, it is found that the operation point has much effect on the performance of SVC when detailed characteristics are considered. The main work is outlined as following, and validated by IEEE 14-bus test system.

(1) When detailed characteristics are considered, SVC operation point has much effect on its steady-state performance.

(2) The system strength to voltage control is repressed as the contribution of slowly Var devices to voltage change, which is applied to restore operation point of SVC while keeping desirable voltage.

(3) The controllable voltage variation and the

feasible slope setting without violation to control limit are quantified based on available control margin at current operation point.

Quantitative analysis and control to SVC operation point is valuable for effective utilization of its control margin and coordination among SVCs and the slow-response Var devices.

References

1) Mathur R.M., Varma R.K., 2002, Thyristor-Based FACTS Controllers for Electrical Transmission Systems, IEEE/Wiley Press.

2) Lee R.L., Beshir M.J., Finley A.T., et al, 1995, Application of Static Var Compensators for the Dynamic Performance of the Mead-Adelanto and Mead-Phoenix Transmission Projects, IEEE Trans. Power Del., 10, No. 1, pp.459–466.

3) Palma-Behnke R., Vargas L.S., Perez J.R., et al, 2004, OPF with SVC and UPFC Modeling for Longitudinal Systems, IEEE Trans. Power Syst., 19, No. 4, pp. 1742–1753.

4) Ambriz-Pérez H., Acha E., Fuerte-Esquivel C., 2000, Advanced SVC Models for Newton-Raphson Load Flow and Newton Optimal Power Flow Studies, IEEE Trans. Power Syst., 15, No. 1, pp.129–136.

5) Taylor C., Scott G., Hammad A., et al, 1994, Static Var Compensator Models for Power Flow and Dynamic Performance Simulation, IEEE Trans. Power Syst., 9, No. 1, pp. 229–240.

6) Hingorani N.G., Gyugyi L., 2000, Understanding FACTS: Concepts and Technology of Flexible AC Transmission Systems, IEEE Press.

7) Kundur P., 1993, Power System Stability and Control, McGraw-Hill Press

Received August 25, 2006
Accepted October 12, 2006